ORIGINAL ARTICLE

Analysis of the influence of the effective angles on the tool wear in gear hobbing

Felix Kühn[1] · Christoph Löpenhaus[1] · Jens Brimmers[1] · Fritz Klocke[1] · Thomas Bergs[1]

Abstract

Gear hobbing is one of the most productive manufacturing processes for cylindrical spur gears. The macro geometry of the cutting edge of a hob depends on the tool angles. The tool angles consist of rake angle, wedge angle, and clearance angle. Due to the relative motion between workpiece and tool, the tool angles change to the effective angles during the process. The tool angles have a significant influence on the abrasive flank wear and the heat transfer through the tool. The use of indexable insert hobs compared to conventional hobs offers geometric design freedom. In contrast to full profile tools, the tool clearance angle can be designed freely along the profile by using indexable insert hobs. By dividing the reference profile into at least one left and one right indexable insert, the rake angles of both flanks can be set independently. As a result, the use of indexable insert hobs offers a significantly increased variability in tool design. In order to predict tool wear, the influences of tool angle and cutting edge geometry on tool wear in gear hobbing with indexable insert must be investigated in more detail. Therefore, the objective of the investigation presented in this paper is to improve the cutting conditions by modifying the effective angles in indexable insert hobbing. In analogy tests, the influence of the effective angle on tool wear was investigated by a variation of the rake and clearance angles. Based on the outcomes of the theoretical and empirical investigation, a wear model was developed for the main wear mechanism of abrasive wear. The wear model was trained by analyzing the tool life through an analogy test and was validated in an industrial hobbing process with indexable inserts.

1 State of the Art

With the fly-cutting trial, Sulzer [20] developed an analogy trial for gear hobbing. The hob is replaced by a fly cutter with the same reference profile as the hob. During the cutting process, the fly-cutter maps all generating positions of the hob in each gap. The fly-cutter trial is successfully used to investigate tool life and wear characteristics in gear hobbing [20].

Winkel [21] used the fly-cutter trial to be carried out systematic wear studies to optimize the tool design for hobs made of carbide. For his experiments, he used the fly-cutter test developed by Sulzer. Winkel carried out tests to modify the tool pressure angle, to prepare defined cutting edges, to

optimize the coating system, and to select the carbide substrate. Winkel did not investigate the tool angles or the effective tool angles [21].

Brecher [4] developed the penetration simulation software SPARTApro to simulate the gear hobbing process. With SPARTApro, characteristic values such as the maximum chip thickness $h_{cu,max}$, the maximum chip length $l_{cu,max}$, and machined volume V' can be calculated. These characteristic values are important for the determination of mechanical and the thermal loads at the cutting edge of the tool. As a next step, SPARTApro was further developed by Klocke [15] to calculate the effective tool angles in the hobbing process [4, 15].

Karpuschewski [13] showed in his investigations that carbide hobs can also be used at high cutting velocities up to $v_c = 800$ m/min and chip thicknesses up to $h_{cu,max} = 0.26$ mm. Karpuschewski explained the wear phenomena with the use of FEM simulation. In addition, he verified the transferability of the fly-cutting trial to the hobbing process. The same wear conditions occurred on the fly cutter at comparable positions as on the full hob [13].

✉ Felix Kühn
  f.kuehn@wzl.rwth-aachen.de

[1] WZL of RWTH Aachen University, Campus-Boulevard 30,
     52074 Aachen, Germany

In further investigations, Karpuschewski [12] analyzed the influence of the tool profile on the tool wear in gear hobbing. In his trials, he investigated the influence of the module, the tip radius, the profile height, and the protuberance on the tool wear. Based on the results, he developed geometrical load parameters to predict tool wear. Karpuschewski did not investigate tool angles [12].

Rech [19] investigated the influence of the cutting edge preparation on tool wear in gear hobbing with fly-cutting trials. In his experiments, a cutting edge radius of $r = 10$ to 20 μm proved to be the optimum. However, Rech did not deal with tool angles in his investigations [19].

Claudin [5] developed an analogy test for gear hobbing by using an entire single flute of a hob. This allows the test to be conducted on a five-axis milling machine. In these trials, Claudin investigated the influence of the cutting edge radius on tool wear; the tool angles were not varied [5].

Antoniadis [1] quantitatively investigated the influence of different process and tool parameters on the fatigue life expectations of cemented carbide tools used for gear hobbing. The lifetime prognosis of the tools, however, was only evaluated for failure due to fatigue fracture. A tool life prognosis for abrasive flank wear was not part of the research. The tool angles remained changed as part of the tool parameter [1].

Hoffmeister [9] identified the effective tool angles as a factor influencing the flank wear in hobbing. For this purpose, single tests were carried out with different design flank clearance angles in the fly-cutting process. It was found that with identical effective clearance angles, an approximately equal wear mark width was achieved. At different effective clearance angles, small clearance angles led to the largest flank wear. Hoffmeister concluded that the effective clearance angles had to be increased to reduce wear. To achieve this, the designed clearance angles must be increased [9].

Joppa [10] investigated the influence of the designed clearance angle on tool wear in hobbing. Joppa carried out fly-cutting trials with three different designed flank clearance angles $\alpha_f = 4°$, $\alpha_f = 5°$, and $\alpha_f = 6°$. By increasing the clearance angle, Joppa determined less wear. As with turning and milling, a larger clearance angle has a positive effect on tool wear, due to lower friction and the associated lower heating. The clearance angle should not be too large so that the cutting wedge is not weakened too much. However, the clearance angle downward is limited by two aspects. Firstly, by the relationship between the tip clearance angle and the flank clearance angle relevant for regrinding and secondly by the effective clearance angle being smaller than the designed clearance angle. To prevent the effective clearance angles from becoming zero or negative, the designed clearance angle should not be too small [10].

Bouzakis [2] investigated the influence of effective clearance and rake angles on tool wear in hobbing. Bouzakis carried out fly-cutting trials with tools made of S 6-5-2-5.

Bouzakis assumed that the wear-reducing effect of a larger effective clearance angle and the wear-inducing effect of a smaller effective rake angle cancel each other out on the leading flank. This is also the situation in the reverse case at the trailing flank. The development of wear on the cutter tooth is therefore not dependent on the effective tool angles, but only on the chip shape, chip thickness, and chip length. Bouzakis confirmed this hypothesis with two different tests, in which he observed the development of wear in the transition from the tip to the leading and trailing flank. Bouzakis could show an influence on the wear behavior if the effective clearance angle becomes smaller than $\alpha_w = 1°$ [2].

Mundt [17] developed a tool life prediction model for gear hobbing. The resulting chip parameters, such as the mean chip thickness, are calculated using approximation functions. In fly-cutting trials, chip parameters were varied to determine the tool life. The geometry parameters on the hob were kept constant [17].

The work of Bouzakis [3] focused on the prediction of wear and the wear behavior of hobs. One objective was to achieve an even wear distribution on the hobs using a tangential shift strategy. For the analysis of tool wear, in addition to the maximum flank wear VB_{max}, the chip parameters cutting length and chip thickness are used. However, an absolute tool life was not determined [3].

Hipke [11] investigated the wear behavior of PM-HSS tools in dry hobbing with high cutting velocities as a function of gear material and gear geometry. On the basis of the investigation, a regression model for calculating the tool life was determined, and a guideline value recommendation for calculating the tool life when hobbing with PM-HSS tools was developed [11].

A reduction of the cutting force due to increased rake angles could be observed by Gunay [7] for turning. The rake angle was varied in steps of 2.5° from $\gamma = -5$ to $\gamma = 12.5°$. As the rake angle increased, a decrease of the cutting force was observed. The cutting force between a rake angle $\gamma = 0$ and $\gamma = 2.5°$ and between $\gamma = 10$ and $\gamma = 12.5°$ decreased the most with up to 3.4%. The cutting force remained almost constant between a rake angle of $\gamma = 2.5°$ and $\gamma = 10°$ [7].

Dahlmann [6] investigated the influence of the rake angle on the residual stresses with the workpiece for turning. An increased negative rake angle resulted in a higher compressive strength. [6]

2 Objective and approach

The objective of the investigations presented in this paper is the improvement of the tool life by optimizing the effective tool angles in gear hobbing with regard to the occurring load. With the manufacturing simulation SPARTApro, characteristic values and the effective tool angles were calculated. Based

on the characteristic values and on empirical findings, a wear model for the dominant wear mechanism, abrasion, of the indexable insert hob was developed. In subsequent analogy trial, the influence of the effective angles on tool wear was investigated by varying the rake and clearance angles. The wear model was trained by analyzing the tool life through an analogy trial.

3 Process kinematics at the idealized cutting wedge

Definitions, nomenclatures, and descriptions for the geometry of a tool cutting wedge are specified in the DIN 6581 [18]. The ideal cutting wedge is represented in Fig. 1, which is composed of tool clearance angle α, wedge angle β, and rake angle γ. The correlation between the clearance, tool, and rake angles is described in the Eq. (3-1).

$$\alpha + \beta + \gamma = 90° \qquad (3-1)$$

α [°]　　Clearance angle
γ [°]　　Rake angle
β [°]　　Wedge angle

The clearance angle influences the heat transfer into the tool. The larger the clearance angle, the smaller is the wedge angle at constant rake angle, which leads to a reduction of the tool tip's stability. If the clearance angle is too large, the transfer of heat can be too severe, increasing the tool temperature and leading to a disturbance or loss of the tool hardness. A small clearance angle improves the heat transfer through the tool. However, if the angle is too small, the contact area between the tool clearance surface and the workpiece surface increases. The friction from this contact leads to abrasive wear with negative effect on the tool life.

The rake angle influences the material forming, which occurs during the cutting process. The larger the rake angle, the smaller is the chip deformation during cutting. On the other hand, the increase of the rake angle reduces the tool stability. The smaller the rake angle, the larger is the chip deformation. In this case, the chip experiences a larger curvature than usual. Due to this, the rake angle influences the resulting cutting forces as well as the temperature along the cutting edge and the rake surface.

In order to have a clear description of location, position, and movement direction of a cutting wedge, a reference system is used, where characteristic planes are defined and applied to all process variants. The two reference systems used are the tool-in-hand system and the tool-in-use system. The tool-in-hand system is used for tool design, as well as for the manufacturing and testing of cutting tools. In this system, the tool angles are measured without considering the process kinematics. During the machining process, the effective clearance and rake angles may differ from the designed angles due to the process kinematics. The tool angle remains unmodified. For this reason, the tool-in-use system was created.

Figure 1 presents the tool-in-use system defined by the effective velocity, which is the result of the vectorial summation of the cutting velocity and the feed rate velocity. The effective clearance angle α_w calculated in the tool-in-use system is smaller than the tool clearance angle α. The wedge angle β remains unmodified. Since the relationship stipulated by Eq. (3-1) is also valid for the tool-in-use system, the variation between the designed rake angle γ and the effective rake angle γ_w is the same amount as the variation of the clearance angle, but in positive direction. In this case, the effective rake angle γ_w is larger than the designed rake angle γ.

Fig. 1 Process kinematics at the idealized cutting wedge

Legend

- Designed tool angles
  - α　: Clearance angle
  - β　: Wedge angle
  - γ　: Rake angle
- Normal effective plane
- Calculation of:
  - Tool angle
    - α_w : Effective clearance angle
    - γ_w : Effective rake angle
  - Working length l_e
  - Chip thickness h_{cu}
- Definitions according to DIN 6580 und DIN 6581
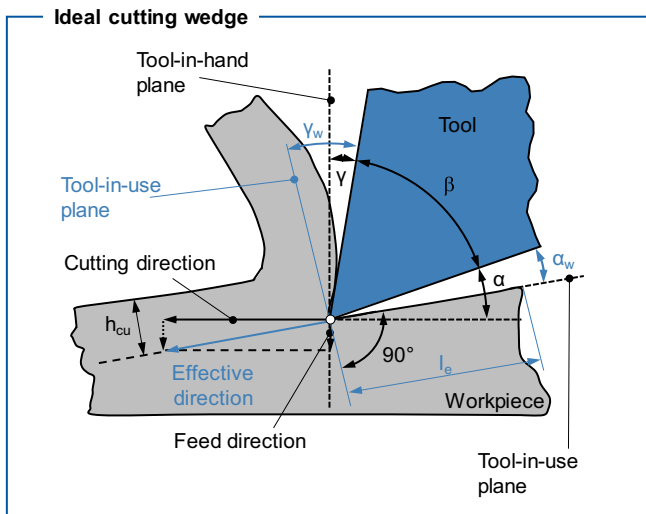
4 Wear trials with variation of tool angles

The tool wear investigations were carried out using an established analogy trial for gear hobbing, the fly cutting trial. In this analogy trial, the entire hob is replaced by one single tooth. During the process, the fly cutter realizes all generating positions of the hob in each gap. The test setup is shown in Fig. 2. The fly-cutting trials are carried out on a GLEASON Pfauter P400 hobbing machine. All machine axes have a direct drive. The cutting spindle has a power rating of 17 kW. The machine was developed for a nominal module of $m_n =$ 8 mm and a maximum workpiece diameter of $d_a = 400$ mm.

The cutting substrate used was carbide K30/HB30F and was coated with an ALCrN coating. The carbide consists of 90% tungsten carbide and 10% cobalt binder phase. The workpiece material was a case-hardened steel 18CrNiMo7-6. The chemical composition was determined by optical emission spectrography (oes) and is shown in Fig. 3.

The tool is a single start, right-hand hob with an outer diameter $d_{a0} = 154.6$ mm, module of $m_n = 8$ mm, $n_{i0} = 12$ number of gashes, and a protuberance of $pr_{p0} = 0.24$ mm. To investigate the influence of the effective tool angles on the tool wear in gear hobbing, the design of experiments was set up as shown in Fig. 4. The workpiece regarded in these investigations has a module $m_n = 8$ mm, a number of teeth $z_2 = 25$, a pressure angle of $\alpha_{n2} = 20°$, a helix angle of $\beta_2 = 0°$, a gearing width of $b = 60$ mm, and an outside diameter $d_{a2} = 220.26$ mm.

The specific adjustment of the effective tool angles is set via the relative velocity v_w between tool and workpiece and the designed tool angle. The designed tool angles are ground into the tool. In order to cover a big range of variations, the designed tool angles were varied. Commonly used tool angles of hobs have a tip clearance angle of $\alpha_k = 10°$ and a gash helix angle of $\gamma_N = 0°$. The usual tool geometry $\alpha_k = 10°$ and $\gamma_N = 0°$ were used as a reference point in the design of experiments.

The helix angle of the fly cutter results in a flank rake angle of $\gamma_f = -3.6°$ for the basic tool.

Two investigation criteria were focused in the design of the experiment. First, by reducing the clearance angle α_k, abrasive flank wear should be investigated. A cutting velocity of $v_c = 225$ m/min was used. Abrasive wear is the dominant wear in gear hobbing with carbide. Due to the high temperature strength of the carbide cutting material in combination with the substrate coating, temperature triggered wear phenomena such as crater wear is not critical. Second, the stability of the cutting edge was investigated by varying the flank rake angle γ_f. To vary the flank rake angle γ_f, the gash helix angle γ_N was varied upwards and downwards. Due to a higher cutting velocity of $v_c = 300$ m/min, the cutting edge was exposed to higher thermal loads. The axial feed rate $f_a = 2.5$ mm and the resulting maximum chip thickness according to Hoffmeister, $h_{cu,max} = 0.34$ mm was kept constant throughout in the trials. The given clearance angles refer to the tip clearance angles α_k.

Before carrying out the experimental investigation, the process for the tool-workpiece combination was analyzed theoretically. The manufacturing simulation SPARTApro was used. Based on the input information regarding tool geometry, workpiece geometry, and process parameters, the tooth gap is generated with the assistance of a numerical penetration calculation. During the simulation, the final chip geometry is determined. The chip geometry characteristic values such as maximum chip thickness $h_{cu,max}$, maximum chip length l_{max}, and machined volume V' can be calculated. These characteristics values are important for the determination of mechanical and thermal loads at the cutting edge of the tool.

The characteristic values resulting from the simulation, the mean chip thickness $h_{cu,m}$, the maximum chip thickness $h_{cu,max}$, the number of cuts, and the maximum chip length $l_{cu,max}$ are shown in Fig. 5 over the unrolled tool profile. The negative area of the unrolled tool profile represents the leading flank and the positive area the trailing flank.
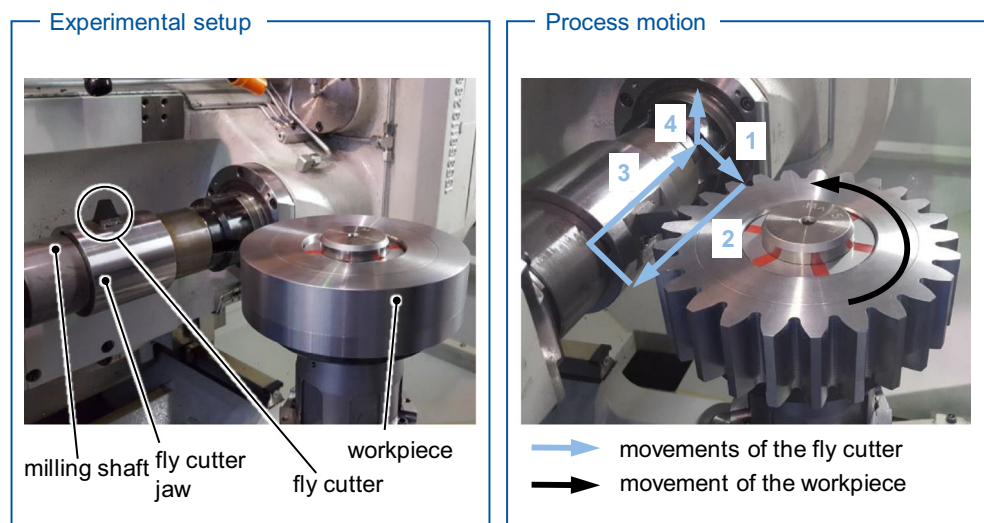
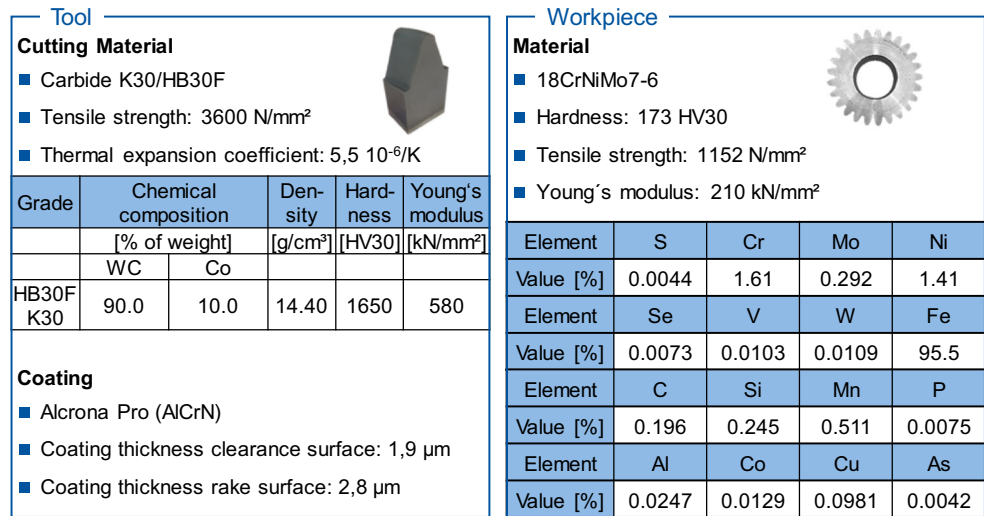**Fig. 2** Experimental setup and process motion

milling shaft fly cutter jaw workpiece fly cutter

movements of the fly cutter
movement of the workpiece

Fig. 3 Tool and workpiece characterization

Tool					
Cutting Material					
■ Carbide K30/HB30F					
■ Tensile strength: 3600 N/mm²					
■ Thermal expansion coefficient: 5,5 10^{-6}/K					
Grade	Chemical composition		Den-sity	Hard-ness	Young's modulus
	[% of weight]		[g/cm³]	[HV30]	[kN/mm²]
	WC	Co			
HB30F K30	90.0	10.0	14.40	1650	580
Coating					
■ Alcrona Pro (AlCrN)					
■ Coating thickness clearance surface: 1,9 µm					
■ Coating thickness rake surface: 2,8 µm					

Workpiece				
Material				
■ 18CrNiMo7-6				
■ Hardness: 173 HV30				
■ Tensile strength: 1152 N/mm²				
■ Young´s modulus: 210 kN/mm²				
Element	S	Cr	Mo	Ni
Value [%]	0.0044	1.61	0.292	1.41
Element	Se	V	W	Fe
Value [%]	0.0073	0.0103	0.0109	95.5
Element	C	Si	Mn	P
Value [%]	0.196	0.245	0.511	0.0075
Element	Al	Co	Cu	As
Value [%]	0.0247	0.0129	0.0981	0.0042

The mean and maximum chip thickness as well as the maximum chip length assume a maximum in the tip area. A maximum chip thickness $h_{cu,max} = 0.36$ mm and a maximum chip length $l_{cu,max} = 57.35$ mm are achieved. The chip thickness and chip length on both sides assume a local minimum in the area of the transition from protuberance to flank. Most cuts are made in the area of the transition from the tip to the protuberances. The transition from the tip to the protuberance of the leading flank completes about 100 cuts more than the transition from the tip to the protuberance of the trailing flank.

From the characteristic values, the tip and the transition to protuberance can be identified as wear critical. The high cutting lengths lead locally to high temperatures and promote abrasive wear. The large chip thicknesses result in high mechanical loads in the tip area. The high number of cuts in the transition from the tip to the protuberance leads to high thermal and mechanical loads and thus accelerated wear process in this area. The transition area is therefore important for the examination criterion of cutting edge stability. The process

parameters shown are not influenced by the cutting velocity or the design tool angles, so that the characteristic values remain unchanged in all trials carried out.

Figure 6 shows the designed clearance angles α and effective clearance angles α_w along the unrolled tool profile as well as the wear curves for the trial points of $\alpha_k = 10°$, $\alpha_k = 6°$, and $\alpha_k = 2°$. The required tip clearance angles could not be produced exactly and result to the tip clearance angles of $\alpha_k = 10.59°$, $\alpha_k = 6.04°$, and $\alpha_k = 2.6°$.

For hobbing, the effective tip clearance angle α_{kw} is the same as the designed tip clearance angle α_k. The feed velocity v_a is negligibly small in relation to the cutting velocity v_c and therefore has no visible influence on the effective velocity v_w. The cutting velocity v_c is perpendicular to the tool reference plane and therefore has no influence on the effective velocity v_w. Thus, the effective tip clearance angles α_{kw} do not differ from the designed tip clearance angles α_k.

A difference between the effective and designed clearance angles becomes visible on the flanks. The effective flank

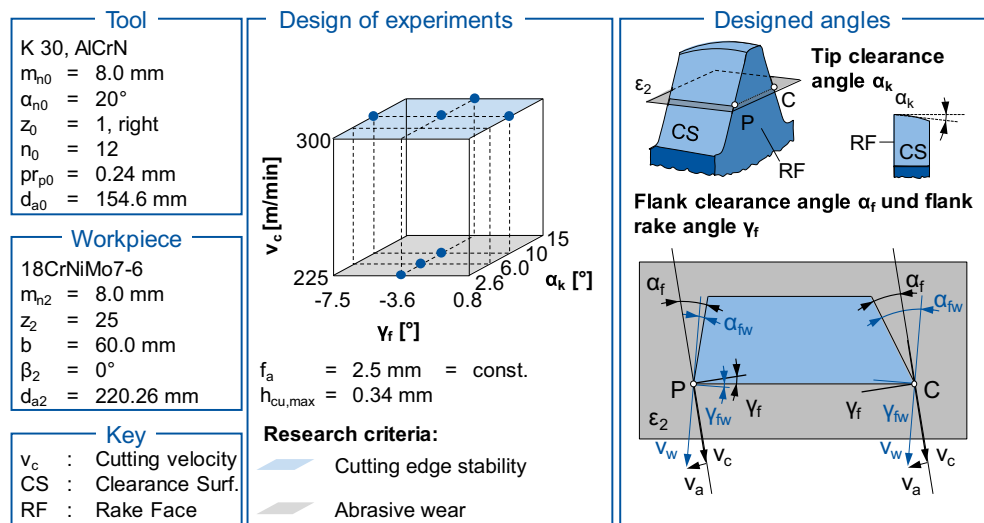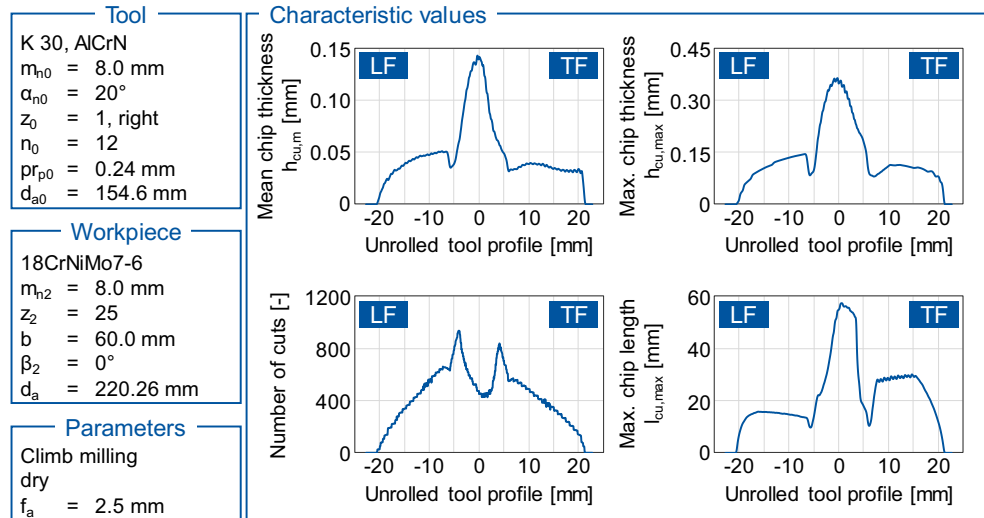**Fig. 4** Tool parameters, workpiece parameters, and design of experiments

Tool
K 30, AlCrN
m_{n0} = 8.0 mm
α_{n0} = 20°
z_0 = 1, right
n_0 = 12
pr_{p0} = 0.24 mm
d_{a0} = 154.6 mm

Workpiece
18CrNiMo7-6
m_{n2} = 8.0 mm
z_2 = 25
b = 60.0 mm
β_2 = 0°
d_{a2} = 220.26 mm

Key		
v_c	:	Cutting velocity
CS	:	Clearance Surf.
RF	:	Rake Face

Design of experiments

f_a = 2.5 mm = const.
$h_{cu,max}$ = 0.34 mm

Research criteria:
◣ Cutting edge stability
▨ Abrasive wear

Designed angles

Fig. 5 Calculated characteristics values with the manufacturing simulation SPARTApro


clearance angle α_{fw} decreases on the leading flank, and the effective flank clearance angle α_{fw} increases on the trailing flank compared to the designed flank clearance angle α_f. The change is caused by the rotation of the workpiece, which changes the effective velocity. For the tools $\alpha_k = 10°$, $\alpha_k = 6°$, and $\alpha_k = 2°$, an effective flank clearance angle of $\alpha_{fw} = 3.95°$, $\alpha_{fw} = 2.20°$ or $\alpha_{fw} = 0.45°$ is produced on the leading flank, and an effective flank clearance angle of $\alpha_{fw} = 4.76°$, $\alpha_{fw} = 2.94°$, or $\alpha_{fw} = 1.76°$ is produced on the trailing flank.

The test series were carried out at a cutting velocity of $v_c = 225$ m/min. The measured amounts of wear are plotted over the corresponding tool life. For determining the end of tool life, a usual value of the maximum flank wear of $VB_{max} = 120$ μm was chosen. The wear was measured by light microscopy using a Keyence VHX-6000 microscope. The tool $\alpha_k = 10°$ reached the end of tool life after $L = 31.5$ m, the tool $\alpha_k = 6°$ after $L = 36$ m, and the tool $\alpha_k = 2°$ after $L = 21.5$ m. All three tools have failed due to flank wear on the tip area or chipping on the cutting edge on the tip area.

In the tip area, the highest loads occur on the cutting edge. The maximum chip thickness and the maximum chip length assume maximum values in the tip area. A higher chip thickness results in higher cutting forces, which can lead to chipping and cutting edge breakouts. The maximum chip length leads to longer contact times between the cutting edge and the workpiece. Longer contact times result in higher temperatures at the cutting edge. During the contact time, the tool is in contact with the workpiece, which leads to abrasive flank wear.

The maximum flank wear VB_{max} only occurred locally at the cutting edge. In order to evaluate the influence of the effective tool angles on the tool wear, the mean flank wear VB was evaluated. The wear curves for the mean flank wear VB are shown in Fig. 6. On the clearance surface of the tip, the leading and trailing flank, a decrease of the mean flank wear VB with increasing effective clearance angles α_w was observed. Increasing the effective clearance angle resulted in a smaller contact area between tool and workpiece. The smaller contact surface favors the abrasive wear.

Fig. 6 Wear development with different clearance angles α
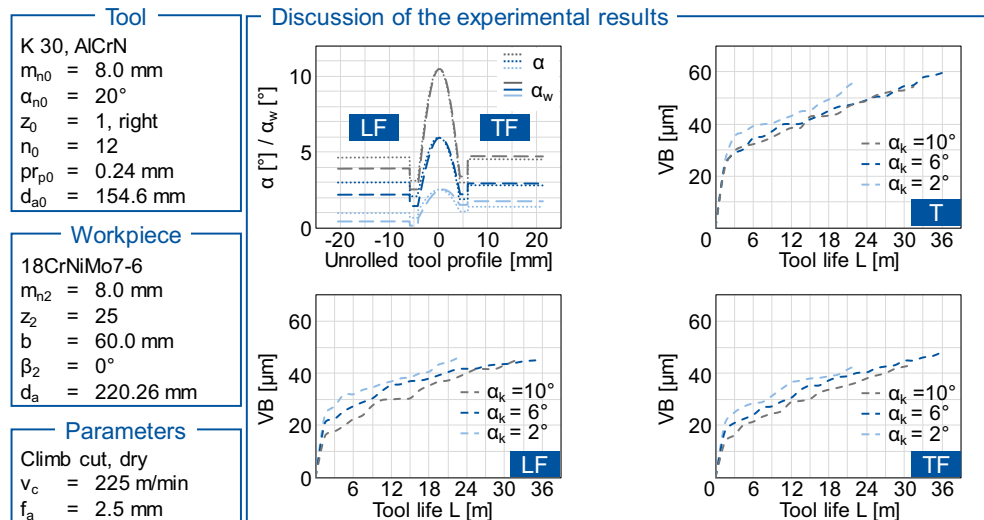
A more precise analysis of the wear is possible with the aid of the microscopic images of the cutting edges shown in Fig. 7. The worn cutting edges of the tools with the different clearance angles are shown. For each tool, the tip area (T), the leading flank (LF), and the trailing flank (TF) are shown. For comparability, all wear images are shown with a tool life of $L = 21.5$ m. The abrasive flank wear is clearly visible. Wear occurs evenly along the cutting edge of all tools. The areas, where the coating is removed and the substrate is exposed, are clearly visible. In the dark area below the wear, elements were detected from the workpiece material 18CrNiMo7-6. Below the dark area, the coating AlCrN is visible. The flank wear of all tools is largest in the tip area. The amount of wear increases as the effective clearance angle increases. The wear images show the same result as the wear curves.

Figure 8 shows the results of the investigations with different flank rake angles $\gamma_f = -7.5°$, $\gamma_f = -3.6°$, and $\gamma_f = 0.8°$, related to the leading flank. The cutting velocity is $v_c = 300$ m/min. The end of the tool life with $\gamma_f = -7.5°$ was reached after $L = 18$ m by a break-out.

The tool with a flank rake angle of $\gamma_f = -3.6°$ also failed after $L = 18$ m through a chipping. For the tool with a flank rake angle of $\gamma_f = 0.8°$, the tip broke off after $L = 21$ m. In the tip area, the flank rake angle γ_f has no geometric influence, since it only changes the flank area. Therefore, the focus is on the wear progression of the leading and trailing flank. The wear curves VB_{max} of the tools with $\gamma_f = -3.6°$ and $\gamma_f = 0.8°$ flank rake angles are almost identical on the leading and trailing flanks. The tool with a flank rake angle of $\gamma_f = -7.5°$ has a larger initial wear than the other two tools. However, the gradients of the wear curves are similar. The curves of VB are on a comparable level for all three tools. In summary, it can be stated that the investigated flank rake angles γ_f have no major influence on tool wear in gear hobbing. However, the flank rake angle γ_f could serve as an adjustment parameter for the specific chip flow direction, whereby chip packing and the resulting tool breakage can be avoided.

The wear development of all trials of the design of experiments is summarized in Fig. 9. The maximum width of flank wear VB_{max} and the average width of flank wear VB are applied over the tool life L. The effective clearance angles are applied over the unrolled tool profile. The trials were carried out at two different cutting velocities $v_c = 225$ m/min and $v_c = 300$ m/min. The tools with tip clearance angles $\alpha_k = 2°$, $\alpha_k = 6°$, and $\alpha_k = 10°$ were used at cutting velocity $v_c = 225$ m/min, and the tools with tip clearance angles $\alpha_k = 10°$ and $\alpha_k = 15°$ and flank rake angles $\gamma_f = -7.5°$ and $\gamma_f = 0.8°$ were used at cutting velocity $v_c = 300$ m/min. The wear progressions show that of all factors, the cutting velocity has the biggest influence on the tool life. A higher cutting velocity leads to a higher thermal load on the cutting edge. The cutting edge impacts the workpiece at a higher speed, resulting in a higher impulse load, which can lead to breakouts of the cutting edge. The tests with cutting velocity $v_c = 300$ m/min show a tool life of approx. $L = 18$ m. All tools with $v_c = 300$ m/min have failed due to chipping of the cutting edge. Chipping can be attribute to tool errors, inhomogeneity's in the material or cutting material, or to defects in the coating. Thus, chipping of the cutting edge is often a statistical phenomenon. All tests with $v_c = 300$ m/min failed after a similar tool life with a chipping. Chipping of the cutting edge is not reproducible forms of wear. For this reason, the average width of flank wear VB was analyzed in the following to develop a process model for local tool wear. The maximum chip thickness according to Hoffmeister with $h_{cu,max} = 0.34$ mm is very unusual for the cutting material. In industrial environments, the maximum chip thickness according to Hoffmeister is designed to $h_{cu,max} = 0.2$ mm for carbide tools. For the trials, the maximum chip thickness was selected to $h_{cu,max} = 0.34$ mm, as no significant increase of wear occurred in preliminary tests with lower maximum chip thicknesses $h_{cu,max}$.

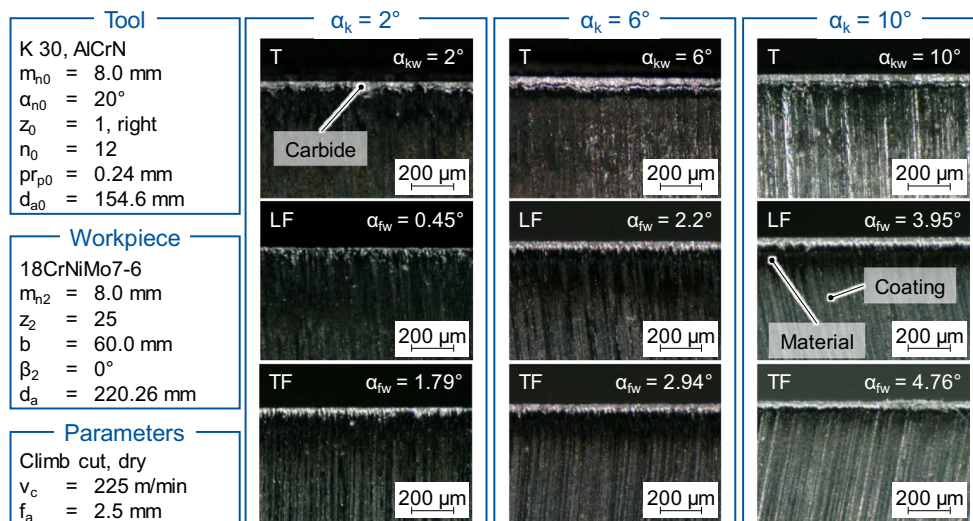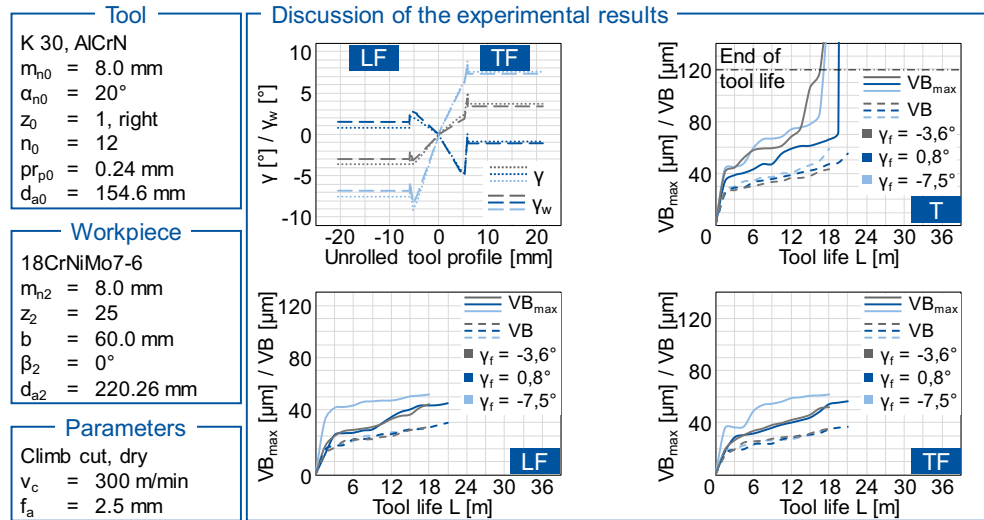**Fig. 7** Wear images for the different clearance angles α

**Fig. 8** Wear development with different rake flank angles γ_f

The trials with a cutting velocity of $v_c = 225$ m/min achieved a tool life of approx. $L = 30$ m, which results in an increase in tool life of 66%. Only the tool with the lowest tip clearance angle of $\alpha_k = 2°$ achieved a tool life of $L = 22.5$ m. The difference in tool life is due to the small clearance angle. The maximum chip thickness $h_{cu,max}$ has remained constant compared to the trials with the higher cutting velocity v_c. It could be shown that in the trials, higher chip thicknesses can be set for carbide than recommended in the literature.

5 Tool wear modelling

After the fly-cutter tests with different effective tool angles, a wear characteristic value Kv was developed, which allows to calculate the abrasive flank wear along the tool profile. Abrasive wear increases in the machining process with increasing machined length. The cutting energy also increases

with increasing length. For this reason, an energy approach was used for wear modelling. To establish the energy approach, the assumption was made that a contact surface is created between the material and the tool clearance surface. The contact surface is formed by the elastic material deformation immediately after the machining process. In the local view, the three-dimensional contact surface becomes a two-dimensional contact length l_k. In addition to the contact length, the thrust force F_D and the tool life L are important for the formation of abrasive wear of the flank. The thrust force acts perpendicular to the cutting direction and acts in the same direction as the assumed main elastic deformation. In the local view, the thrust force is related to the chip width and is referred to as the relative thrust force F_D'. To establish the energy approach, the contact length l_k, the relative thrust force F_D', and the tool life L were taken as elementary components and linked according to equation (5-1). The constants a and c take into account the combination of tool substrate and

Fig. 9 Wear development of all fly-cutter trials
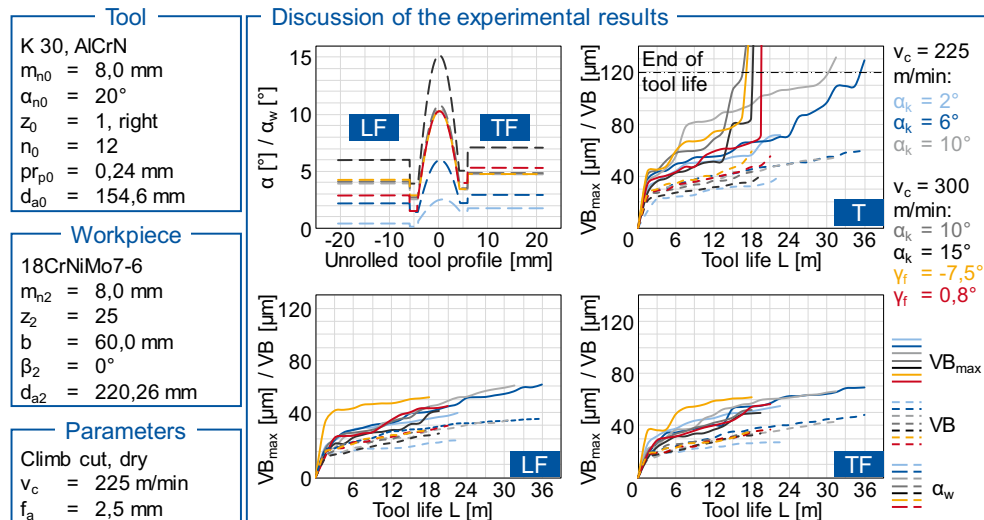
material. The empirically determined constants for the cutting material combination of carbide and 18CrNiMo7-6 used result in $a = 0.66$ m^{-c} and $c = 0.35$.

$$\mathrm{Kv} = l_k \cdot F_D{}' \cdot a \cdot L^c \qquad (5-1)$$

Kv [Nm]   Wear characteristic value
$F_D{}'$ [N/m]   Relative thrust force
L [m]   Tool life
l_k [m]   Contact length
a [m$^{1\text{-}c}$]   Tool substrate and material coefficent
c [−]   Tool substrate and material coefficent

Friction between the tool clearance surface and the workpiece is an important influencing factor for the formation of abrasive flank wear. The forces occurring on the tool during machining are the cutting force F_c and the thrust force F_D. The direction of the cutting force F_c is antagonistic to the cutting velocity v_c, and the thrust force F_D pushes the tool away from the workpiece. The forces are applied from the workpiece to the tool. If the forces are considered from the tool to the workpiece, the sign of the forces is reversed. Figure 10 shows the forces acting on the workpiece by the tool. The thrust force F_D deforms the workpiece elastically along the clearance surface of the tool, creating a contact of a length of l_k between the clearance surface of the tool and the workpiece. This contact length l_k, see equation (5-2), depends on the effective clearance angle α_w, the thrust force F_D, and the Young's modulus of the material.

$$l_k = \sqrt{\frac{F_D{}' \cdot l_z}{\sin\alpha_w \cdot \cos\alpha_w \cdot E}} \qquad (5-2)$$

l_k [m]   Contact length
l_z [m]   Tooth thickness
E [N/m^2]   Young's modulus
$F_D{}'$ [N/m]   Specific thrust force
α_w [°]   Effective clearance angle

The thrust force can be calculated according to Gutmann for gear hobbing [8]. The force calculation according to Gutmann was applied in several works and further developed to increase the accuracy [14, 16]. The contact length l_k can be calculated by inserting the equations (5-4) to (5-7) into Equation (5-3).

$$E = \frac{\sigma}{\varepsilon} \qquad (5-3)$$

$$\sigma = \frac{F}{A} = \frac{F'}{l_k} \qquad (5-4)$$

$$\varepsilon = \frac{\Delta l_z}{l_z} \qquad (5-5)$$

$$\Delta l_z = l_k \cdot \sin\alpha_w \qquad (5-6)$$

$$F' = \frac{F_D{}'}{\cos\alpha_w} \qquad (5-7)$$

E [N/m^2]   Young's modulus
ε [−]   Deformation
A [m^2]   Surface
l_k [m]   Contact length
l_z [m]   Tooth thickness
$F_D{}'$ [N/m]   Specific thrust force
σ [N/m^2]   Normal stress
F [N]   Normal force
F' [N/m]   Specific normal force
Δl_z [m]   Deformation length
α_w [°]   Effective clearance angle

The wear characteristic value Kv is shown in Figure 11 over the unrolled tool profile for the trials with the tip clearance angles $\alpha_k = 6°$, $\alpha_k = 10°$ with $v_c = 225$ m/min and $\alpha_k = 10°$, $\alpha_k = 15°$ with $v_c = 300$ m/min. The diagram also shows the mean width of flank wear VB after $L = 15$ m for the same trial points above the unrolled tool profile. The focus is on the mean width of flank wear VB. The maximum width of flank wear VB$_{max}$ only occurs locally at the cutting edge and is not shown over the unrolled tool profile. The maximum width of flank wear VB$_{max}$ often occurs due to layer damage to the

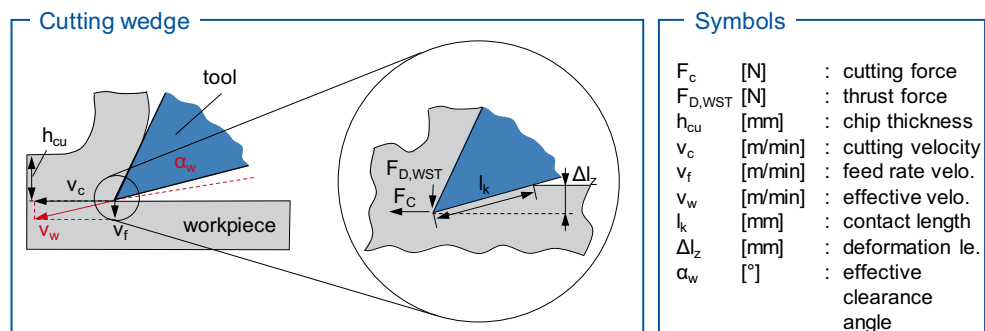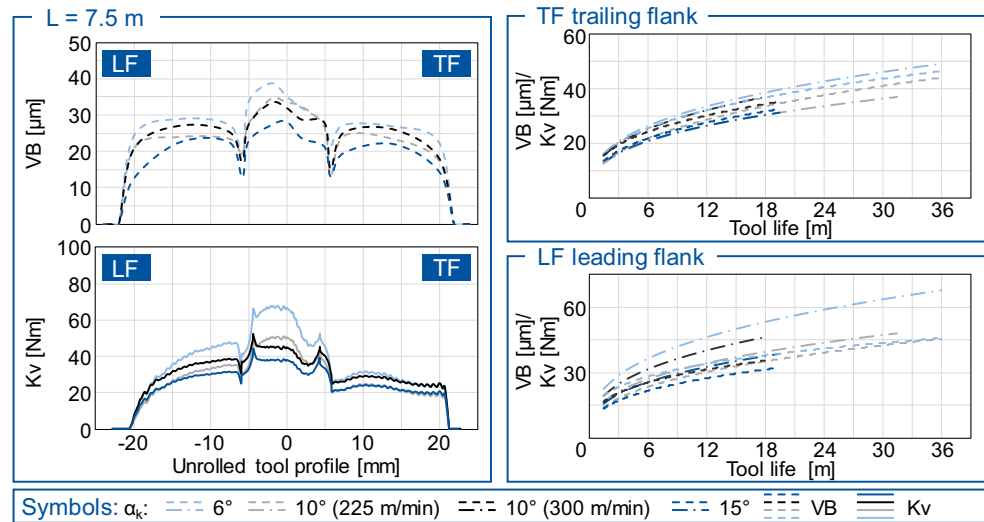**Fig. 10** Contact length l_k between clearance surface and workpiece

Fig. 11 The wear characteristic value Kv

coating or local defects in the cutting material. Statistical influences were not investigated.

The wear characteristic value Kv matches the qualitative curve of the mean width of flank wear VB well. The maximum values of the wear characteristic value Kv are, just like the curve of VB, in the left tip area of the profile. The wear on the left side of the profile is bigger than the wear on the right side. This condition is also reflected qualitatively in the wear characteristic value. The difference in size between the flank areas and the tip area is also displayed correctly in the wear characteristic value Kv. In the area of the lower tool profile and in the area of protuberance, the courses of the wear characteristic value Kv do not reflect the qualitative course of flank wear with sufficient accuracy. However, since the wear in these areas assumes the lowest wear values and the qualitative progression of the wear characteristic Kv is above the wear progression, these areas are regarded as negligible. The areas where the biggest wear occurs are qualitatively represented by the wear characteristic value Kv.

In addition to flank wear along the unrolled tool profile, the wear characteristic value Kv and the mean width of flank wear VB over the tool life are shown in Fig. 11. The calculated wear progress represents the measured wear progress of the different tests qualitatively well. The gradient of the wear characteristic value Kv over the tool life is comparable to the gradient of the measured wear progress. In the case of the absolute wear, differences can be found between the wear characteristic value Kv and the mean width of flank wear VB. The difference is caused by different initial wear. Initial wear is often characterized by mechanisms such as micro-fractures and flaking of layers, which occur statistically and not systematically. Therefore, the modeling of the initial wear and the exponential range is not possible. As soon as the initial wear changes to a constant wear progress, the wear progress can be modelled by the wear characteristic value Kv and, thus, be concluded on the tool life to be achieved.

For all wear tests, the gradient of the mean width of flank wear VB and the maximum width of flank wear VB$_{max}$ is very

similar for leading and trailing flank, (see Fig. 9). Therefore, the wear characteristic value Kv can also be used to predict the gradient of VB$_{max}$.

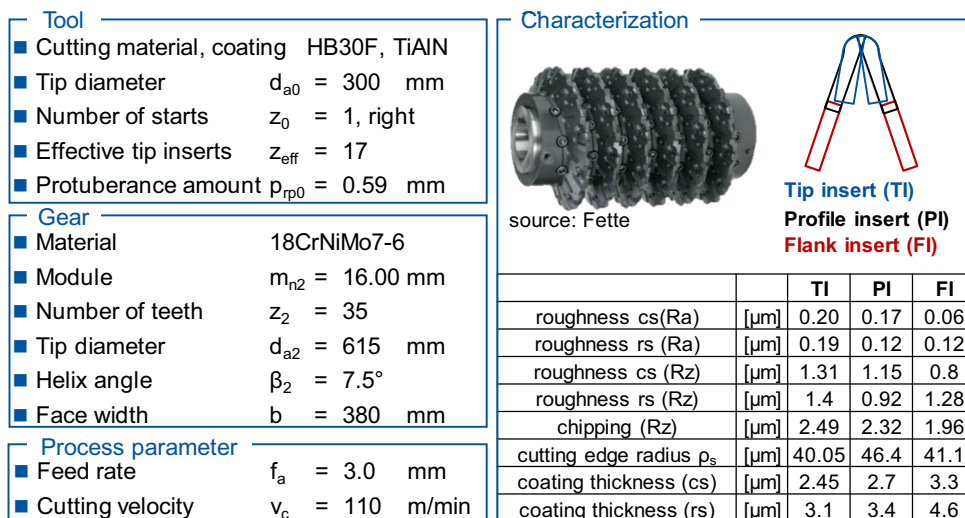## 6 Validation of the wear model

The wear model was applied to an indexable insert hobbing process for the wind power industry. The tool has a tip diameter of $d_{a,0} = 300$ mm, as shown in Fig. 12. The indexable inserts are consisting of K30/HB30F carbide and are coated with TiAlN coating. The tool profile is represented by six cutting sections. The division of the cutting sections is symmetrical to the profile center line.

The test gear is a planetary gear with a module of $m_n = 16$ mm, a pressure angle of $\alpha_n = 20°$, a helix angle of $\beta = 7.5°$ and a tip diameter of $d_{a,2} = 615$ mm. The gear is made of the steel alloy 18CrNiMo7-6 and has $z_2 = 35$ teeth.

The maximum chip thickness and the effective clearance angle were calculated. Figure 13 shows the effective clearance angle over the unrolled tool profile. The tool has a designed clearance angle of $\alpha_f = 3.7°$ on the left and right flank and $\alpha_k = 9.5°$ in the tip area of the cutting edge. The effective clearance angle on the left flank is smaller than the designed clearance angle with an amount $\alpha_{fw} = 3°$. On the right flank, the effective clearance angle is bigger than the designed clearance angle. The effective and designed clearance angle in the tip area are both $\alpha_{kw} = \alpha_k = 9.5°$. The smallest clearance angles are achieved in the area of protuberance.

Wear trials were carried out with the presented tool and the mean width of flank wear VB and the maximum width of flank wear VB$_{max}$ were recorded consecutively through a microscope. The progress of flank wear is exemplary shown for the right tip indexable inserts, for the right upper flank indexable inserts, and for the right lower flank indexable inserts in Fig. 13 over the tool life.

Fig. 12 Tool and gear characterization

Tool
- Cutting material, coating　HB30F, TiAlN
- Tip diameter　d_{a0} = 300　mm
- Number of starts　z_0 = 1, right
- Effective tip inserts　z_{eff} = 17
- Protuberance amount　p_{rp0} = 0.59　mm

Gear
- Material　18CrNiMo7-6
- Module　m_{n2} = 16.00 mm
- Number of teeth　z_2 = 35
- Tip diameter　d_{a2} = 615　mm
- Helix angle　β_2 = 7.5°
- Face width　b = 380　mm

Process parameter
- Feed rate　f_a = 3.0　mm
- Cutting velocity　v_c = 110　m/min

Characterization

source: Fette

Tip insert (TI)
Profile insert (PI)
Flank insert (FI)

		TI	PI	FI
roughness cs(Ra)	[μm]	0.20	0.17	0.06
roughness rs (Ra)	[μm]	0.19	0.12	0.12
roughness cs (Rz)	[μm]	1.31	1.15	0.8
roughness rs (Rz)	[μm]	1.4	0.92	1.28
chipping (Rz)	[μm]	2.49	2.32	1.96
cutting edge radius ρ_s	[μm]	40.05	46.4	41.1
coating thickness (cs)	[μm]	2.45	2.7	3.3
coating thickness (rs)	[μm]	3.1	3.4	4.6

In addition, the wear progress was modelled with the help of wear characteristic value Kv and also applied over the tool life. Since the gradients of the wear curves of the maximum width of flank wear VB_{max} and the mean width of flank wear VB differ considerably, especially from a tool life of 25 m, the maximum width of flank wear VB_{max} was used to validate the more wear-critical course. In Fig. 13, the curve of wear is represented by a trend curve. The calculated curve of the wear characteristic value Kv shows the trend curve of the measured wear curve qualitatively well. The amount differences between the calculated and measured gradients are again due to the non-modellable initial wear. Due to the good match of the model and the trials, the wear characteristic value Kv can be regarded as validated.

7 Conclusion

The objective of the investigation is to improve cutting conditions by modifying the effective tool angles in hobbing. The use of indexable insert hobs compared to conventional hobs offer geometric design freedom. In contrast to full profile tools, the designed clearance angle along the profile is virtually free when using indexable insert hobs. With this design, the fixed relationship between tip and right and left flank clearance angles is not necessary. By splitting the reference profile on at least one left and one right indexable insert, the rake angles of both flanks can be set independently. This means that the use of indexable insert hobs results in a significantly increased possibility of variation in tool design.

For a large gear with a module of $m_{n2} = 8$ mm, the effective tool angles were calculated, and fly cutting trials were carried out with different clearance and rake angles. The designed clearance angle was varied within the production limits from $\alpha_k = 2°$ to $\alpha_k = 15°$. The rake angle was varied within the limits $\gamma_f = -7.5°$ to $\gamma_f = 0.8°$, which corresponds to a gash helix angle of $\gamma_N = -4.5°$ to $\gamma_N = 4.5°$. Two investigation criteria were analyzed for the design of the experiment. On the one hand, abrasive wear should be investigated by

Fig. 13 Validation of the wear model
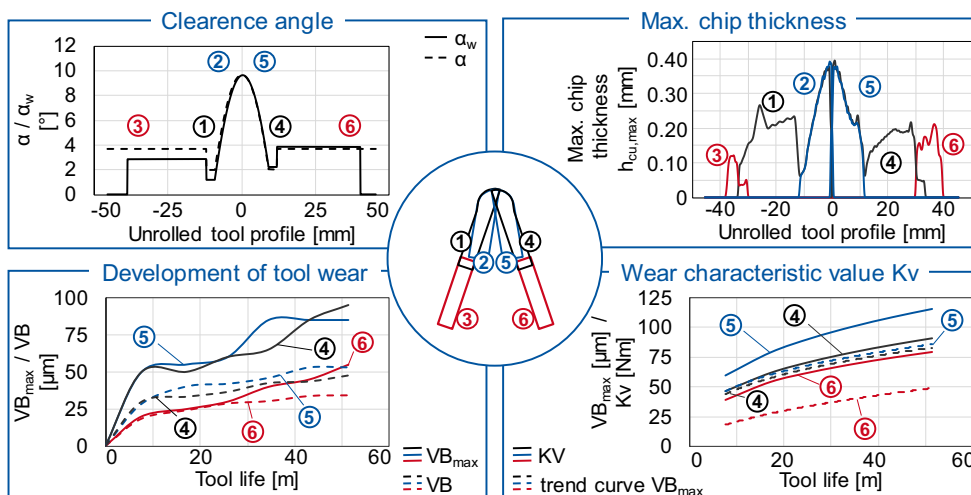
reducing the clearance angle α_k. On the other hand, the stability of the cutting edge was investigated by varying the flank rake angle γ_f. The measured flank wear was applied over the tool life. The tool life criterion was set to $VB_{max} = 120$ µm.

In summary, it can be stated that in all trials which carried out a larger effective clearance angle α_w led to a reduction of the flank wear. Increasing the effective clearance angle resulted in a smaller contact area between tool and workpiece. The smaller contact surface favors the abrasive wear.

The investigated flank rake angles γ_f did not show any significant influence on tool wear in gear hobbing. However, the flank rake angle γ_f could serve as an adjustment parameter for the specific chip flow direction, whereby chip packing and the resulting tool breakage can be avoided.

The results of the fly-cutting trials were used to develop a wear model for abrasive flank wear for different tool angles. With this model, it is possible to predict the wear along the tool profile and along the tool life qualitatively.

The calculation method and the wear model were validated for a $m_{n2} = 16$ mm indexable insert hob. It was shown that the effective tool angles, machining parameters, and the wear curves can be calculated.

References

1. Antoniadis A, Vidakis N, Bilalis N (2002) Fatigue fracture investigation of cemented carbide tools in gear hobbing. Part 2: the effect of cutting parameters on the level of tool stresses - a quantitative parametric analysis. J Manuf Sci Eng (124):792–797

2. Bouzakis K-D (1981) Konzept und technologische Grundlagen zur automatisierten Erstellung optimaler Bearbeitungsdaten beim Wälzfräsen. Habil.-Schr., RWTH Aachen University

3. Bouzakis K-D, Lili E, Michailidis N, Friderikos O (2008) Manufacturing of cylindrical gears by generating cutting processes. A critical synthesis of analysis methods. CIRP Ann Manuf Technol 57(2):676–696

4. Brecher C, Brumm M, Krömer M (2015) Design of gear hobbing processes using simulations and empirical data. Procedia CIRP 33: 484–489. https://doi.org/10.1016/j.procir.2015.06.059

5. Claudin C, Rech J (2009) Development of a new rapid characterization method of hob's wear resistance in gear manufacturing—application to the evaluation of various cutting edge preparations in high speed dry gear hobbing. J Mater Process Technol 209(11): 5152–5160. https://doi.org/10.1016/j.jmatprotec.2009.02.014

6. Dahlmann P, Gunnberg F, Jacobson M (2004) The influence of rake angle, cutting feed and cutting depth on residual stresses in hard turning. J Mater Process Technol (147):181–184

7. Günay M, Aslan E, Korkut I, Seker U (2004) Investigation of the effect of rake angle on main cutting force. Int J Mach Tool Manu 44:953–959

8. Gutmann P (1988) Zerspankraftberechnung beim Wälzfräsen. Diss., RWTH Aachen University

9. Hoffmeister B (1970) Über den Verschleiß am Wälzfräser. Diss., RWTH Aachen

10. Joppa K (1978) Bedeutung der effektiven Freiwinkel beim Wälzfräsen. Ind Anz 100(46):32–33

11. Karpuschewski B, Knoche H-J, Hipke M, Beutner M (2012) High performance gear hobbing with powder-metallurgical high-speed-steel. CIRP Conf High Perform Cut 1:196–201

12. Karpuschewski B, Beutner M, Köchig M, Härtling C (2017) Influence of the tool profile on the wear behaviour in gear hobbing. CIRP J Manuf Sci Technol

13. Karpuschewski B, Beutner M, Köchig M, Wengler M (2017) Cemented carbide tools in high speed gear hobbing applications. CIRP Ann Manuf Technol 66:117–120

14. Klocke F, Schröder T, Schalaster R (2007) Cutting forces and tool wear in dry high-speed hobbing of different workpiece materials. In: Brecher C, Klocke F (Hrsg) 2nd WZL Gear Conference in the USA

15. Klocke F, Löpenhaus C, Kühn F (2018) Analysis of the influence of the working angles on the tool wear in gear hobbing. Gear Technol 35(1):56–66

16. Kühn F, Löpenhaus C, Klocke F (2016) Further development of a cutting force model for gear hobbing. Adv Mater Res (1140):165–172

17. Mundt A (1992) Modell zur rechnerischen standzeitbestimmung beim Wälzfräsen. Diss., RWTH Aachen

18. Norm (1985) Begriffe der Zerspantechnik. Bezugssysteme und Winkel am Schneidteil des Werkzeuges (6581). Beuth, Berlin

19. Rech J (2006) Influence of cutting edge preparation on the wear resistance in high speed dry gear hobbing. Wear 261:505–512

20. Sulzer G (1973) Leistungssteigerung bei der Zylinderradherstellung durch genaue Erfassung der Zerspankinematik. Diss., RWTH Aachen University

21. Winkel O (2005) Steigerung der Leistungsfähigkeit von Hartmetallwälzfräsern durch eine optimierte Werkzeuggestaltung. Diss., RWTH Aachen